

Superposition rheology

Jan K. G. Dhont¹ and Norman J. Wagner²

¹Forschungszentrum Jülich, IFF, Weiche Materie, D-52425 Jülich, Germany

²Colburn Laboratory, Department of Chemical Engineering, University of Delaware, Newark, Delaware 19716

(Received 4 August 2000; published 26 January 2001)

The interpretation of superposition rheology data is still a matter of debate due to lack of understanding of viscoelastic superposition response on a microscopic level. So far, only phenomenological approaches have been described, which do not capture the shear induced microstructural deformation, which is responsible for the viscoelastic behavior to the superimposed flow. Experimentally there are indications that there is a fundamental difference between the viscoelastic response to an orthogonally and a parallel superimposed shear flow. We present theoretical predictions, based on microscopic considerations, for both orthogonal and parallel viscoelastic response functions for a colloidal system of attractive particles near their gas-liquid critical point. These predictions extend to values of the stationary shear rate where the system is nonlinearly perturbed, and are based on considerations on the colloidal particle level. The difference in response to orthogonal and parallel superimposed shear flow can be understood entirely in terms of microstructural distortion, where the anisotropy of the microstructure under shear flow conditions is essential. In accordance with experimental observations we find pronounced negative values for response functions in case of parallel superposition for an intermediate range of frequencies, provided that microstructure is nonlinearly perturbed by the stationary shear component. For the critical colloidal systems considered here, the Kramers-Kronig relations for the superimposed response functions are found to be valid. It is argued, however, that the Kramers-Kronig relations may be violated for systems where the stationary shear flow induces a considerable amount of new microstructure.

DOI: 10.1103/PhysRevE.63.021406

PACS number(s): 82.70.Dd, 05.70.Jk, 51.20.+d, 64.60.Ht

I. INTRODUCTION

Superposition rheology is a tool to investigate the internal dynamics of stationary sheared systems. At present there are a number of phenomenological models [1–3], but no microscopic theory exists where response functions are obtained from considerations on the particle level. *It is the purpose of this paper to develop a microscopic theory for superposition rheology.* The system that will be considered is a *concentrated system of attractive, spherical colloids in the vicinity of the gas-liquid critical point.* Explicit results are obtained for the viscoelastic response functions related to a weak shear field superimposed on a (possibly strong) stationary shear field. Interesting phenomena are observed when the stationary shear field is strong enough to perturb the microstructure in a nonlinear fashion. To some extent these microscopic considerations lead to an intuitive understanding of superimposed response.

Some of the commonly used phenomenological models violate the Kramers-Kronig relations [1,2]. It will be argued that the Kramers-Kronig for the superimposed response functions are valid for systems in which the stationary shear flow does not lead to a considerable enhancement of microstructure. For systems where shear flow leads to a considerable enhancement of microstructure, the Kramers-Kronig might be violated. Such a violation might be found for entangled polymer systems, or systems close to the gel transition. For the near-critical system considered here, however, microstructural distortion is dominant over microstructural enhancement, and the Kramers-Kronig relations are found to apply.

This paper is organized as follows. First of all we outline the basic steps that go into microscopic theories for vis-

coelastic behavior. Although the structure of a microscopic theory for viscoelastic behavior of colloids has been discussed by many authors before, we feel that a short expose here is worthwhile, since this paper will be of interest to rheologists who are probably not familiar with these issues. After having defined the flow geometry in Sec. III, the superposition rheology of attractive spheres near their gas-liquid critical point, where many-body interactions are essential, is treated in extenso in Sec. IV. In Sec. IV A some introductory remarks on the critical divergence of the viscosity are given for those rheologists who are not familiar with critical phenomena. Sec. IV B is concerned with the effect of shear flow on the microstructure of the suspension, Sec. IV C discusses a microscopic expression for the viscoelastic response functions, and Sec. IV D contains explicit results and an interpretation of the difference of response functions for parallel and orthogonal superposition. In Sec. V the validity of the Kramers-Kronig relations for stationary sheared systems is discussed. Section VI contains some concluding remarks.

II. THE BASIC STEPS IN A MICROSCOPIC THEORY

A microscopic theory for viscoelastic behavior consists of three steps:

(i) Calculate the probability density function (PDF) $P \equiv P(\mathbf{r}_1, \dots, \mathbf{r}_N)$ of the position coordinates $\{\mathbf{r}_j | j = 1, 2, \dots, N\}$ of the spherical colloidal particles for the system subjected to flow. The PDF P obeys the so-called Smoluchowski equation, which reads [4–6],

$$\frac{\partial P}{\partial t} = D_0 \sum_{j=1}^N \nabla_j \cdot [\nabla_j P + \beta P \nabla_j \Phi] - \sum_{j=1}^N \nabla_j \cdot [\Gamma \cdot \mathbf{r}_j P], \quad (1)$$

where hydrodynamic interactions between colloidal particles are neglected. Here, D_0 is the single-particle diffusion coefficient, ∇_j is the gradient operator with respect to \mathbf{r}_j , and Φ is the total interaction energy of the assembly of N colloidal particles. Furthermore, Γ is the velocity gradient tensor, which will be specified in the next section. This is a diffusion equation that includes direct interactions between the colloidal particles (through the potential Φ), their Brownian motion (second term between the square brackets) and convective motion (through the last term). It is a microscopic equation of motion since it is formulated on the level of the colloidal particles. The first task is thus to solve this equation of motion with approximations that are appropriate for the particular system under consideration.

(ii) Find the function f of the position coordinates of the colloidal particles, which upon averaging with respect to the above-mentioned PDF gives the macroscopic viscoelastic response functions, or equivalently, the macroscopic stress, that is,

$$\begin{aligned} \text{stress} &= \langle f \rangle \\ &\equiv \int d\mathbf{r}_1 \dots \int d\mathbf{r}_N f(\mathbf{r}_1, \dots, \mathbf{r}_N) P(\mathbf{r}_1, \dots, \mathbf{r}_N, t). \end{aligned} \quad (2)$$

Such a microscopic expression for the stress has been derived in full generality by Batchelor [7]. In Sec. IV C we will give an elementary derivation that applies to near critical systems.

(iii) Evaluate the average in Eq. (2). Once steps (i) and (ii) are accomplished, one should then evaluate the integral (2) to find, for example, the shear rate dependence of the viscoelastic response functions. In most cases the explicit evaluation relies in part on numerical integration.

The function in Eq. (2), which upon averaging gives the stress, is generally a sum of functions $f(\mathbf{r}_i - \mathbf{r}_j)$ of two position coordinates only. For identical colloidal particles we then have (the summation ranges over $i \neq j$),

$$\begin{aligned} \text{stress} &= \int d\mathbf{r}_1 \dots \int d\mathbf{r}_N \sum_{i,j=1}^N \mathbf{f}(\mathbf{r}_i - \mathbf{r}_j) P(\mathbf{r}_1, \dots, \mathbf{r}_N, t) \\ &= \frac{N(N-1)}{V^2} \int d\mathbf{r}_1 \int d\mathbf{r}_2 \mathbf{f}(\mathbf{r}_1 - \mathbf{r}_2) g(\mathbf{r}_1 - \mathbf{r}_2, t), \end{aligned} \quad (3)$$

where V is the volume of the system and g is the pair-correlation function, which is defined as

$$g(\mathbf{r}_1 - \mathbf{r}_2, t) \equiv V^2 \int d\mathbf{r}_3 \dots \int d\mathbf{r}_N P(\mathbf{r}_1, \mathbf{r}_2, \mathbf{r}_3, \dots, \mathbf{r}_N, t). \quad (4)$$

This pair-correlation function $g(\mathbf{r}, t)$ is thus proportional to the probability to find two colloidal particles a distance $\mathbf{r} = \mathbf{r}_1 - \mathbf{r}_2$ apart. Step (i) is now reduced to finding the shear rate dependent pair-correlation function g . Note that by definition $g(\mathbf{r}) \rightarrow 1$ as $r \rightarrow \infty$.

Since the deviatoric part of the stress in an isotropic system vanishes, we can write the integral in Eq. (3) also as,

$$\text{stress} = \frac{N(N-1)}{V} \int d\mathbf{r} h(\mathbf{r}) f(\mathbf{r}), \quad (5)$$

where $h \equiv g - 1$ is referred to as the total-correlation function. This function vanishes at infinity. The reason for introducing the total-correlation function is that it is often easier to solve equations for the structure factor $S(\mathbf{k})$, which is essentially the Fourier transform of $h(\mathbf{r})$,

$$S(\mathbf{k}) = 1 + \bar{\rho} \hat{h}(\mathbf{k}), \quad (6)$$

where $\bar{\rho} = N/V$ is the number density of colloidal particles and with $\hat{h}(\mathbf{k})$ the Fourier transform of $h(\mathbf{r})$,

$$\hat{h}(\mathbf{k}) = \int d\mathbf{r} h(\mathbf{r}) \exp\{i\mathbf{k} \cdot \mathbf{r}\}. \quad (7)$$

The Fourier transform of $h(\mathbf{r})$ is well defined since $h(\mathbf{r})$ vanishes at infinity, contrary to the pair-correlation function. Parseval's theorem allows one to rewrite the stress (3) in terms of a wave-vector integral,

$$\text{stress} = \frac{N(N-1)}{V(2\pi)^3} \int d\mathbf{k} \hat{h}(\mathbf{k}) \hat{f}(\mathbf{k}), \quad (8)$$

where $\hat{f}(\mathbf{k})$ is the Fourier transform of $f(\mathbf{r})$. It is therefore generally sufficient to find an expression for the (shear-rate dependent) structure factor in order to evaluate the response functions.

Another motivation to calculate the structure factor is that it is of direct relevance for scattering experiments. The predicted shear induced anisotropy and the shear-rate and time dependence of the structure factor can be verified by means of light scattering experiments.

III. THE FLOW FIELD

The *stationary* flow field considered here is a simple shear flow in the x direction with its gradient component in the y direction. The *superimposed oscillatory* shear flow is either parallel to the stationary shear flow or orthogonal to it. The velocity \mathbf{u} at a point \mathbf{r} is $\mathbf{u}(\mathbf{r}) = \Gamma \cdot \mathbf{r}$, with Γ the velocity gradient tensor. This tensor is equal to $\Gamma = \Gamma_0 + \Gamma_s$ with Γ_0 the velocity gradient tensor pertaining to the stationary shear component of the flow and Γ_s to the superimposed velocity gradient tensor. For the above described stationary flow we have

$$\Gamma_0 = \dot{\gamma} \begin{pmatrix} 0 & 1 & 0 \\ 0 & 0 & 0 \\ 0 & 0 & 0 \end{pmatrix}, \quad (9)$$

while for parallel superposition,

$$\Gamma_s = \dot{\gamma}_s \cos\{\omega t\} \begin{pmatrix} 0 & 1 & 0 \\ 0 & 0 & 0 \\ 0 & 0 & 0 \end{pmatrix}, \quad (10)$$

and for orthogonal superposition,

$$\Gamma_s = \dot{\gamma}_s \cos\{\omega t\} \begin{pmatrix} 0 & 0 & 0 \\ 0 & 0 & 0 \\ 0 & 1 & 0 \end{pmatrix}, \quad (11)$$

where the shear flow is in the z direction. Here, $\dot{\gamma}$ and $\dot{\gamma}_s$ are the shear rates corresponding to the stationary and oscillatory component of the flow, respectively. The oscillatory shear rate $\dot{\gamma}_s$ is assumed small enough to assure a linear viscoelastic response, while the shear-rate $\dot{\gamma}$ of the stationary component may perturb the systems microstructure in a nonlinear fashion.

These forms of the velocity gradient tensors assume that frequencies are small enough to assure that the penetration depth is of the order or larger than the gapwidth. We do not consider surface loading experiments. Microstructural dynamics of near-critical systems is very slow, due to critical slowing down, which enables one to perform bulk experiments at frequencies much larger than typical inverse microstructural relaxation times.

IV. SHEARED SUSPENSIONS OF ATTRACTIVE SPHERES NEAR THEIR GAS-LIQUID CRITICAL POINT

A gas-to-liquid transition in a monodisperse suspension of spherical colloidal particles can occur when the pair-interaction potential has a sufficiently strong attractive component. On approach of the corresponding gas-liquid critical point the range of the effective interaction potential diverges. This implies that increasingly larger groups of colloidal particles interact simultaneously on approach of the critical point. The range of the effective interaction potential is measured by the so-called correlation length ξ . The divergence of the range of the effective interaction potential, and hence the number of particles that interact simultaneously, gives rise to divergence of the shear viscosity. Contrary to dilute suspensions, where two-particle interactions are dominant, now many-body interactions are essential.

A. Critical divergence of response functions

The fact that close to the critical point many particles interact simultaneously, gives rise to a large force necessary to break up these interactions in order to make the system flow. This implies a large viscosity, which ultimately diverges at the critical point, since there, each colloidal particle interacts with all other colloidal particles in the system.

Critical divergence resulting from the development of long-range correlations can be understood more formally as follows. As pointed out in Sec. II, the viscosity η can be written as an average as,

$$\eta = \int d\mathbf{r} f(\mathbf{r}) h(\mathbf{r}), \quad (12)$$

where $h(\mathbf{r})$ is the total-correlation function and $f(\mathbf{r})$ is an as yet unknown function of the distance \mathbf{r} between two colloidal particles. At distances r between two colloidal particles, so large that they do not interact with each other any more, the total-correlation function vanishes. The development of long-range correlations means that $h(\mathbf{r})$ goes to zero at large distances more and more slowly. At the critical point its decay to zero at infinity is not sufficiently rapid anymore to assure convergence of the integral in Eq. (12). This is the formal argument why the viscosity diverges at the critical point (like many other transport coefficients). How fast a transport coefficient diverges on approach of the critical point depends solely on the asymptotic behavior of the corresponding phase function $f(\mathbf{r})$ at large distances r . Therefore, for the calculation of the diverging viscosity, only the asymptotic behavior of the function $f(\mathbf{r})$ at large distances is of importance. The contribution to the integral in Eq. (12) resulting from integration over short distances (say r less than a few times the range of the pair-interaction potential) constitutes the so-called ‘‘background viscosity.’’ The remaining contribution to the integral, reflecting the development of long-range correlations, is referred to as the ‘‘anomalous part of the viscosity.’’ The anomalous contribution to the viscosity diverges on approach of the critical point while the background viscosity remains well-behaved. Our interest here is in the anomalous part of the viscoelastic response functions.

B. Microstructure under shear flow

Without shear flow the structure factor attains the Ornstein-Zernike form (see, for example Refs. [6,8]),

$$S^{\text{eq}}(k) = \frac{1}{\beta \Sigma} \frac{\xi^2}{1 + (k\xi)^2}, \quad (13)$$

where $\beta = 1/k_B T$, Σ is a well-behaved, positive constant, which is related to the Cahn-Hilliard square gradient coefficient, and ξ is the correlation length that measures the distance over which colloidal particles still interact with each other. The correlation length is given by,

$$\xi = \sqrt{\Sigma / \frac{d\Pi}{d\bar{\rho}}}, \quad (14)$$

where Π is the osmotic pressure and $\bar{\rho}$ the number density of colloidal particles. Since $d\Pi/d\bar{\rho} \rightarrow 0$ on approach of the critical point, the correlation length diverges, so that the structure factor is infinite for zero wave vectors at the critical point. Close to the critical point the structure factor exhibits a strong upswing at small wave vectors leading to strong forward scattering of light, giving rise to a strong increase of the turbidity. This phenomenon is referred to as ‘‘critical opalescence.’’

The Smoluchowki equation (1) can be integrated with respect to the position coordinates $\mathbf{r}_3, \dots, \mathbf{r}_N$ to obtain an equation of motion for the total-correlation function $h(\mathbf{r}_1 - \mathbf{r}_2)$. Since we are only interested in the asymptotic behavior at large distances, and h vanishes at infinity, the equation of motion can be linearized with respect to h . With an appropriate closure relation for the three-particle correlation function and employing a gradient expansion of h , one finds after Fourier transformation the following equation of motion for the structure factor [6,9,10],

$$\frac{\partial S(\mathbf{k}, t)}{\partial t} = [\dot{\gamma} k_1 + \dot{\gamma}_s \cos\{\omega t\} k_n] \frac{\partial S(\mathbf{k}, t)}{\partial k_2} - 2D^{\text{eff}}(k) k^2 \{S(\mathbf{k}, t) - S^{\text{eq}}(k)\}, \quad (15)$$

where k_j is the j th component of the wave-vector \mathbf{k} , while $k_n = k_3$ for orthogonal superposition and $k_n = k_1$ for parallel superposition, that is,

$$\begin{aligned} n &= 1, & \text{for } \parallel \text{ superposition,} \\ &= 3, & \text{for } \perp \text{ superposition.} \end{aligned} \quad (16)$$

Furthermore, D^{eff} is a diffusion coefficient which is equal to,

$$D^{\text{eff}}(k) = \beta D_0 \left[\frac{d\Pi}{d\bar{\rho}} + k^2 \Sigma \right], \quad (17)$$

where D_0 is the single-particle, Stokes-Einstein diffusion coefficient.

Linearization of the equation of motion for the total-correlation function h amounts to the neglect of terms of order $\mathcal{O}(h^2)$ with respect to a linear term $h \beta d\Pi/d\bar{\rho}$. Very close to the critical point, where $\beta d\Pi/d\bar{\rho}$ is a very small number, such a neglect is no longer allowed. The equation of motion (15) is therefore only valid in the mean-field region, not too close to the critical point. Beyond mean field, very close to the critical point, equations of motion for the structure factor are nonlinear, contrary to Eq. (15). Furthermore, Eq. (15) is valid only for wave vectors k smaller than about $2\pi/R_V$, with R_V the range of the pair-interaction potential, since it relates to the asymptotic form of the total-correlation function for large distances.

The first term on the right-hand side of Eq. (15) describes the distortion of microstructure due to the shearing motion of the suspension and the second term describes the equilibrium restoring diffusion. The relative magnitudes of these two counter balancing terms determine the microstructural features of the system. This competition between convection and diffusion will certainly be modified by hydrodynamic interactions, but the essential features of the microstructure under shear flow are captured without considering hydrodynamic interactions. Inclusion of hydrodynamic interactions is something that remains to be done.

Note that on approach of the critical point, where $d\Pi/d\bar{\rho} \rightarrow 0$, the diffusion coefficient (17) becomes small at small wave vectors. This slowing down of diffusive motion on approach of the critical point is commonly referred to as

“critical slowing down.” As a result of critical slowing down the frequency of the superimposed shear flow, where elastic response will be found, shifts to lower values on the approach of the critical point.

The dimensionless form of Eq. (15) reads,

$$\frac{\partial S(\mathbf{K}, \tau)}{\partial \tau} = [\lambda K_1 + \lambda_s \cos\{\Omega \tau\} K_n] \frac{\partial S(\mathbf{K}, \tau)}{\partial K_2} - K^2 [1 + K^2] \times \{S(\mathbf{K}, \tau) - S^{\text{eq}}(K)\}, \quad (18)$$

where \mathbf{K} is a dimensionless wave vector,

$$\mathbf{K} = \mathbf{k} \xi, \quad (19)$$

and τ a dimensionless time,

$$\tau = 2D^{\text{eff}}(k=0) \xi^{-2} t = 2D_0 \beta \Sigma \xi^{-4} t. \quad (20)$$

This is the time in units of the time required for a colloidal particle to diffuse over a distance equal to the correlation length. Furthermore, the following “dressed Peclet numbers” are introduced,

$$\begin{aligned} \lambda &= \frac{\dot{\gamma} \xi^4}{2D_0 \beta \Sigma} = \frac{\dot{\gamma} \xi^2}{2D^{\text{eff}}(k=0)}, \\ \lambda_s &= \frac{\dot{\gamma}_s \xi^4}{2D_0 \beta \Sigma} = \frac{\dot{\gamma}_s \xi^2}{2D^{\text{eff}}(k=0)}, \end{aligned} \quad (21)$$

and Ω is a dimensionless frequency (or “a dressed Deborah number”),

$$\Omega = \frac{\omega \xi^4}{2D_0 \beta \Sigma} = \frac{\omega \xi^2}{2D^{\text{eff}}(k=0)}. \quad (22)$$

The dimensionless numbers λ and λ_s measure the long-wavelength shear induced distortion of the structure factor resulting from the stationary shear component and the oscillatory component, respectively. The response to the superimposed shear field is linear when $\lambda_s < 1$ and nonlinear when $\lambda_s > 1$. The stationary shear field perturbs the microstructure only slightly when $\lambda < 1$ and in a nonlinear fashion when $\lambda > 1$. A significant phase shift of the structure factor response relative to the external field $\sim \cos\{\omega t\}$ will be found for $\Omega > 1$, while for $\Omega < 1$ the viscous response will be almost instantaneous.

Notice that λ , λ_s , and Ω , for given $\dot{\gamma}$, $\dot{\gamma}_s$, and ω , become larger on approach of the critical point because of the increasing correlation length ξ . The effect of shear flow is thus more pronounced closer to the critical point. This is due to the increasing size ξ of groups of correlated particles on approach of the critical point, which larger groups are more easily affected by shear flow. Furthermore, due to critical slowing down of dynamics, the typical frequency where the response of the structure factor will have an out-of-phase component with the applied oscillatory field, occurs at smaller frequencies ω .

Although the equation of motion (18) can be solved for large values of λ_s , where the viscoelastic response is nonlinear, we restrict ourselves here to small values of λ_s . The general idea is to probe the dynamics of a possible nonlinearly, stationary sheared system with a minimum effect of the superimposed flow. The oscillatory solution of Eq. (18) to linear order in λ_s , after transients have died away, reads,

$$S(\mathbf{K}, \tau) = S^{\text{stat}}(\mathbf{K}) + \frac{\lambda_s K_n}{\lambda K_1} \int_{-\infty}^{\tau} d\tau' \cos\{\Omega\tau'\} G^2(\tau - \tau') \times [1 + G^2(\tau - \tau')] \{S^{\text{stat}}(\mathbf{G}(\tau - \tau')) - S^{\text{eq}}[G(\tau - \tau')]\} \exp\{-H(\tau - \tau')\}, \quad (23)$$

where the vector \mathbf{G} is equal to,

$$\mathbf{G}(\tau - \tau') = [K_1, K_2 + \lambda K_1(\tau - \tau'), K_3], \quad (24)$$

where G is its length, and the function H in the exponent is equal to,

$$H(\tau - \tau') = \int_{\tau'}^{\tau} d\tau'' G^2(\tau - \tau'') [1 + G^2(\tau - \tau'')] = (\tau - \tau') \times [K^2(1 + K^2) + (1 + 2K^2)K_2\lambda K_1(\tau - \tau')] + \frac{1}{3}(1 + 2K^2 + 4K_2^2)\lambda^2 K_1^2(\tau - \tau')^2 + \frac{1}{2}K_2\lambda^3 K_1^3(\tau - \tau')^3 + \frac{1}{5}\lambda^4 K_1^4(\tau - \tau')^4. \quad (25)$$

Here, K_j is the j th component of the dimensionless wave vector (19). Furthermore, $S^{\text{stat}}(\mathbf{K})$ is structure factor under stationary shear flow, without the superimposed oscillatory flow. From the equation of motion (18) with $\lambda_s = 0$ and with the use of Eq. (13) for the equilibrium structure factor, one finds that,

$$S^{\text{stat}}(\mathbf{K}) = S^{\text{eq}}(K) \left[1 + \frac{1}{\lambda K_1} \int_{K_2}^{\pm\infty} dX \times [K^2 - K_2^2 + X^2][K_2^2 - X^2] \exp\left\{-\frac{\mathbf{F}(\mathbf{K}|X)}{\lambda K_1}\right\} \right], \quad (26)$$

where,

$$F(\mathbf{K}|X) = \int_{K_2}^X dY [K^2 - K_2^2 + Y^2][1 + K^2 - K_2^2 + Y^2] = [X - K_2][K^2 - K_2^2][1 + K^2 - K_2^2] + \frac{1}{3}[X^3 - K_2^3][1 + 2K^2 - 2K_2^2] + \frac{1}{5}[X^5 - K_2^5]. \quad (27)$$

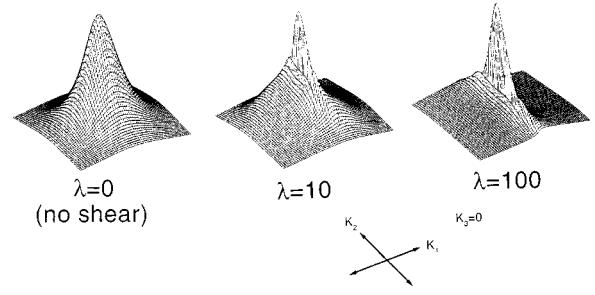


FIG. 1. The structure factor S^{stat} under stationary shear flow as a function of K_1 and K_2 for $K_3 = 0$ (K_1 and K_2 both range from -3 to $+3$). The most left figure is the Ornstein-Zernike equilibrium structure factor. The two other figures are for Peclet numbers $\lambda = 10$ and 100 , respectively.

The upper integration limit in Eq. (26) is equal to $+\infty$ when $\lambda K_1 > 0$, and equal to $-\infty$ when $\lambda K_1 < 0$.

A crucial observation is that *in directions perpendicular to the stationary flow direction (where $K_1 = 0$) the stationary component of the shear flow does not affect the microstructure, that is,*

$$S^{\text{stat}}(\mathbf{K}) = S^{\text{eq}}(K), \quad \text{for } K_1 = 0. \quad (28)$$

As can be seen from Fig. 1, where S^{stat} is plotted for various values of λ in the plane where $K_3 = 0$, the structure factor distortion is highly anisotropic. There is no distortion in directions where $K_1 = 0$, while in the other directions the structure factor is significantly distorted. This will be important when discussing the difference between the response to orthogonal and parallel superimposed shear flow. Contrary to the parallel superimposed shear field, the orthogonal superimposed shear field acts in part on microstructure that is still intact, that is, unaffected by the stationary shear field. This leads to a viscoelastic response to orthogonal flow that is larger than for parallel flow. This is illustrated in Fig. 2, where the additional distortion $S - S^{\text{stat}}$ due to the superimposed oscillatory flow for orthogonal (left column of figures) and parallel (right column) superposition is plotted. The middle column indicates the times during the oscillation at which the structure factor is calculated. All plots refer to cuts in reciprocal space where $K_2 = 1$ (as will be seen later, directions where $K_2 = 0$ do not contribute to the stress). The top two figures are the equilibrium and the stationary sheared structure factor (for $\lambda = 10$). As can be seen, the distortion for orthogonal superposition is about a factor of 10 larger than for parallel superposition. The large distortion in case of orthogonal superposition occurs at wave vectors where the stationary structure factor is equal to the equilibrium structure factor (indicated by the thick line in the top-right plot). *This large susceptibility of the stationary sheared structure factor to orthogonal superimposed flow leads to larger viscoelastic response functions as compared to parallel superimposed flow.*

Except for the factor $\cos\{\Omega\tau'\}$ in Eq. (23), the entire integrand is a function of $\tau - \tau'$ only. Using that,

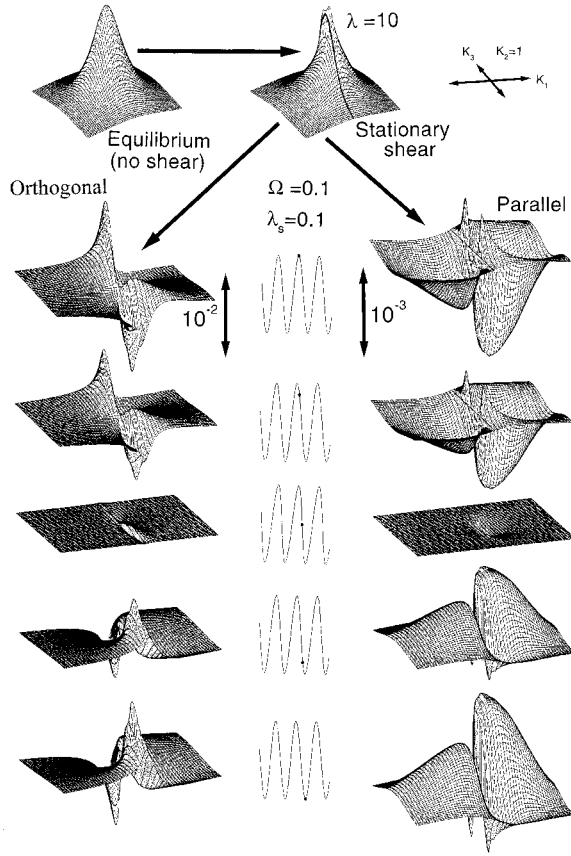


FIG. 2. The structure factor under superimposed oscillatory shear flow in the (K_1, K_3) plane with $K_2=1$. The top left figure is the Ornstein-Zernike equilibrium structure factor, the top right figure is the structure factor under stationary shear flow with a Peclet number $\lambda=10$. The thick line in the latter figure indicates the undistorted structure at $K_1=0$. In these figures both K_1 and K_3 range from -3 to $+3$. The left column of figures is $S - S^{stat}$ for orthogonal superimposed flow for various times. These times are indicated in the middle column by the black dot. Both K_1 and K_3 range from -1 to $+1$. The right column of figures are for parallel flow, where K_1 and K_3 range from -2 to $+2$. Note that the z scale for parallel flow is about factor of 10 smaller than for orthogonal flow, as indicated next to the two top figures in the columns. Here, $\lambda_s = 0.1$, $\Omega = 0.1$, and $\xi^{-1}d = 0.01$.

$$\begin{aligned} \cos\{\Omega\tau'\} &= \cos\{\Omega(\tau' - \tau) + \Omega\tau\} = \cos\{\Omega\tau\}\cos\{\Omega(\tau - \tau')\} \\ &+ \sin\{\Omega\tau\}\sin\{\Omega(\tau - \tau')\}, \end{aligned}$$

allows one to rewrite Eq. (23) explicitly as an in-phase and out-phase contribution to the oscillatory structure factor,

$$\begin{aligned} S(\mathbf{K}, \tau) &= S^{stat}(\mathbf{K}) + \frac{\lambda_s K_n}{(\xi^{-1}d)^2} [F^{in}(\mathbf{K}|\lambda, \Omega)\cos\{\Omega\tau\} \\ &+ F^{out}(\mathbf{K}|\lambda, \Omega)\sin\{\Omega\tau\}], \end{aligned} \quad (29)$$

where d is the core diameter of the colloidal particles and (renaming the new integration variable $\tau - \tau'$ simply as τ),

$$\begin{aligned} \left\{ \begin{array}{l} F^{in}(\mathbf{K}|\lambda, \Omega) \\ F^{out}(\mathbf{K}|\lambda, \Omega) \end{array} \right\} &= \frac{(\xi^{-1}d)^2}{\lambda K_1} \int_0^\infty d\tau \left\{ \begin{array}{l} \cos\{\Omega\tau\} \\ \sin\{\Omega\tau\} \end{array} \right\} G^2(\tau) \\ &\times [1 + G^2(\tau)] \times \{S^{stat}(\mathbf{G}(\tau)) \\ &- S^{eq}(G(\tau))\} \exp\{-H(\tau)\}. \end{aligned} \quad (30)$$

Note that the in- and out-phase functions $F^{in,out}$ are the same for orthogonal and parallel superposition, and are independent of the superimposed shear rate λ_s ; this is the reason for writing the factor $\lambda_s K_n$ explicitly in Eq. (29). The factor $\sim \xi^{-2}$ is added to the definition of the functions $F^{in,out}$ to explicitate the divergence of the structure factors: the functions $F^{in,out}$ are well behaved and independent of the correlation length ξ at the critical point since the structure factors diverge like ξ^2 .

Note that even in the linear-response regime with respect to the stationary component of the flow, where λ is small, there are many relaxation times. For small λ we have, according to Eq. (25), $H(\tau) = \tau K^2(1 + K^2)$, so that every different value of K corresponds to a different relaxation time. In fact these are the different diffusion modes. For stronger stationary flows, where $\lambda > 1$, the additional contributions to H in Eq. (25) are related to coupling between convective and diffusive modes. Even for the simplest colloidal system a Maxwell relaxation model, with a single relaxation time, is generally wrong. Only when the structure is dominated by a nonzero single wave vector, k_m say, there is a dominant single relaxation time $\sim 1/D(k=k_m)k_m^2$, with D the relevant diffusion coefficient. Otherwise there are many relaxation times $\sim 1/D(k)k^2$.

Also note that the equation of motion (18) is singularly perturbed by both the stationary and oscillatory components of the shear flow, with a mathematical boundary layer around $\mathbf{K} = \mathbf{0}$ with a width that varies like the square root of the Peclet numbers. Within the boundary layer, a linearized solution of the equation of motion is a bad approximation, even for small values of the Peclet numbers. It makes sense, however, to use the linearized solution to calculate linear viscoelastic response functions, since in ensemble averages, represented by wave-vector integrals, the boundary layer does not contribute for small Peclet numbers, as its extent vanishes with vanishing Peclet numbers.

The microstructure does not instantaneously adapt to the imposed oscillatory shear field $\sim \cos\{\Omega\tau\}$ when the Deborah number Ω is sufficiently large. This can be seen in Fig. 3, where the structure factor (23) for parallel superimposed flow, normalized to its maximum value, is plotted as a function of time for the wave vector $\mathbf{K} = (1/\sqrt{3}, 1/\sqrt{3}, 1/\sqrt{3})$, for $\lambda = 0.1$ (a linear perturbed microstructure by the stationary component of the flow), $\lambda = 10$ (a nonlinear perturbed microstructure) and $\lambda = 1000$ (a strongly nonlinear perturbed microstructure) for various values of Ω . The external field is given by the dashed curve. In the top row figures (where $\lambda = 0.1$) it is seen that an out-of-phase response becomes evident for $\Omega = 1$. When λ exceeds 1, so that the stationary shear flow perturbs the microstructure in a nonlinear fashion, the microstructure ‘stiffens,’ and an out-of-phase component becomes evident only at frequencies much larger than

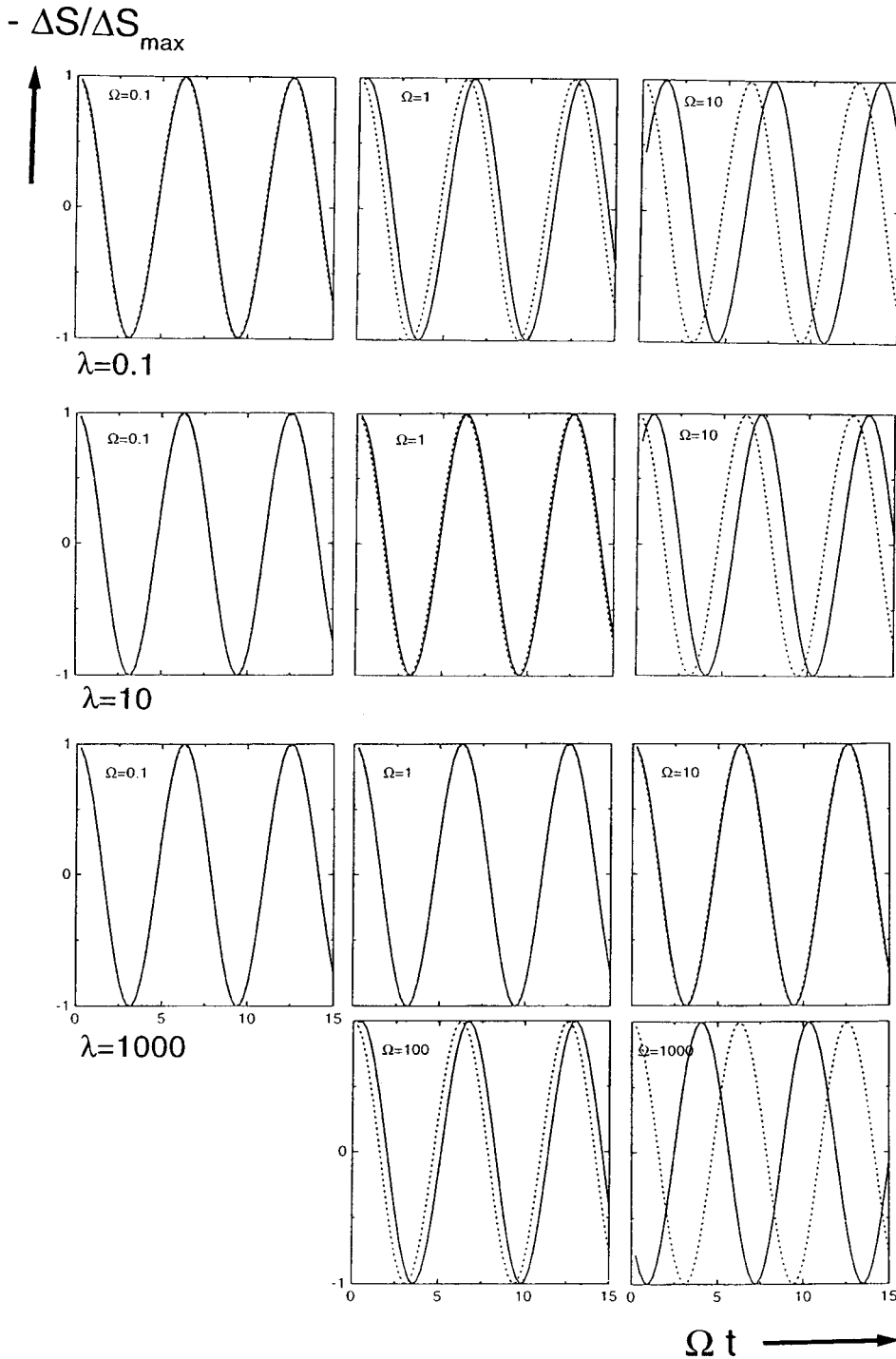


FIG. 3. The additional distortion $-\Delta S = -(S - S^{\text{stat}})$ of the structure factor, resulting from parallel superimposed shear flow (normalized to its maximum value) for the wave vector $\mathbf{K} = (1/\sqrt{3}, 1/\sqrt{3}, 1/\sqrt{3})$ as a function of time for stationary Peclet numbers $\lambda = 0.1$ (top row figures), $\lambda = 10$ (middle row figures), and $\lambda = 1000$ (lower two rows of figures), for various frequencies. Here, $\lambda_s = 0.1$ and $\xi^{-1}d = 0.01$.

1. This is especially evident from the lower two rows of figures, where $\lambda = 1000$. “Stiffening of the microstructure” is due to the fact that larger stationary shear rates destroy microstructures with increasingly larger diffusive relaxation rates. The microstructure, of which the corresponding diffusive relaxation time is sufficiently slow, is no longer present under stationary shear flow. This will, for example, result in an imaginary contribution to the shear viscosity that is almost 0 over a frequency range that increases with increasing stationary shear rates. Once the frequency is substantially larger than λ , an out-of-phase response of the microstructure

becomes evident, leading to a nonzero value of the imaginary part of the shear viscosity.

This effect of “stiffening of microstructure” is less pronounced for orthogonal superposition, since here part of the microstructure that is probed by the superimposed flow is the equilibrium structure [see Eq. (28)]. For parallel superimposed flow this unaffected, equilibrium structure will remain intact, but will be affected by the orthogonally superimposed flow.

For values of the superimposed Peclet number λ_s larger than 1, one finds that the structure factor response is no

longer a (possibly shifted) cosine: higher-order Fourier components now come into play, giving rise to higher-order, nonlinear viscoelastic response functions. These are not considered in the present paper.

C. Microscopic expression for the viscoelastic response functions

To within linear response with respect to the superimposed, oscillatory component of the shear flow, the stress $\sigma(t)$ can be written as,

$$\sigma(t) = \dot{\gamma}_s [\eta'(\omega) \cos\{\omega t\} + \eta''(\omega) \sin\{\omega t\}], \quad (31)$$

which defines the the viscoelastic response functions η' and η'' . This is a valid definition when transients have died away, so that the externally imposed flow field is sinusoidally varying with time. The in-phase response function η' is related to the in-phase part F^{in} of the structure factor in Eq. (30), while the out-phase response function η'' is related to the out-phase part F^{out} .

A microscopic expression for the stress tensor for colloidal systems has been derived by Batchelor [7]. Only the contribution to the stress that arises from interactions between the colloidal particles is of interest here, since only these interactions become long ranged on approach of the critical point. The other terms in Batchelor's expression contribute only to the well-behaved background viscosity. An alternative, elementary derivation of a microscopic expression for the anomalous contribution to the stress proceeds as follows. The dissipated and stored energy \dot{U} per unit volume and unit time, due to the superimposed shear field, is equal to,

$$\dot{U} = \dot{\gamma}_s^2 \cos\{\omega t\} [\eta'(\omega) \cos\{\omega t\} + \eta''(\omega) \sin\{\omega t\}]. \quad (32)$$

On the other hand \dot{U} is proportional to the additional velocity $\Delta \mathbf{V}_j^s$ that colloidal particle j attains as a result of the superimposed field, multiplied by the force \mathbf{F}_j^h that the fluid exerts on that particle (the superscript ‘‘h’’ stands for ‘‘hydrodynamic’’), summed over all particles in the system,

$$\dot{U} = \frac{1}{V} \sum_{j=1}^N \langle \Delta \mathbf{V}_j^s \cdot \mathbf{F}_j^h \rangle, \quad (33)$$

where V is the volume of the system, N the number of colloidal particles, and the brackets $\langle \dots \rangle$ denote averaging with respect to the probability density function (PDF) of the position coordinates of the colloidal particles. Equating the two expressions (32) and (33) one obtains,

$$\begin{aligned} & \dot{\gamma}_s^2 \cos\{\omega t\} [\eta'(\omega) \cos\{\omega t\} + \eta''(\omega) \sin\{\omega t\}] \\ &= \frac{1}{V} \sum_{j=1}^N \langle \Delta \mathbf{V}_j^s \cdot \mathbf{F}_j^h \rangle, \end{aligned} \quad (34)$$

which is the microscopic expression we were after, provided that $\Delta \mathbf{V}_j^s$ and \mathbf{F}_j^h can be expressed in terms of functions that depend only on the position coordinates of the colloidal particles, which then defines the function f in Eq. (5).

The additional velocity consists of two parts. First of all, each particle is carried by the additional fluid flow, which velocity is equal to $\mathbf{\Gamma}_s \cdot \mathbf{r}_j$, with $\mathbf{\Gamma}_s$ the part of the velocity gradient tensor that relates to the superimposed flow field [see Eqs. (10) and (11)]. Secondly, the flow field $\mathbf{\Gamma}_s \cdot \mathbf{r}$ is scattered by the cores of other particles. This scattered flow field affects particle j in its motion and changes its velocity by $\mathbf{C}'_j : \mathbf{\Gamma}_s$, where \mathbf{C}'_j is a third rank tensor, which depends on all the position coordinates of the colloidal particles. The symbol ‘‘:’’ is a double contraction, where the i th component of the vector $\mathbf{C}'_j : \mathbf{\Gamma}_s$ is equal to $\sum_{n,m=1}^3 (C'_j)_{inm} (\Gamma_s)_{mn}$. The proportionality of this contribution with $\mathbf{\Gamma}_s$ is the result of the linearity of the creeping flow equations, which describe the low Reynolds number hydrodynamics in suspensions. Hence,

$$\Delta \mathbf{V}_j^s = \dot{\gamma}_s \cos\{\omega t\} [\hat{\mathbf{\Gamma}}_s \cdot \mathbf{r}_j + \mathbf{C}'_j : \hat{\mathbf{\Gamma}}_s], \quad (35)$$

where $\hat{\mathbf{\Gamma}}_s$ is the velocity gradient tensor in Eqs. (10) and (11) without the prefactor $\dot{\gamma}_s \cos\{\omega t\}$. For the calculation of the anomalous part of the viscoelastic response functions it is sufficient to use the asymptotic form of the ‘‘disturbance tensor’’ \mathbf{C}'_j for large separations of colloidal particles, as was explained in Sec. IV A. This asymptotic form is just the sum of pair contributions,

$$\mathbf{C}'_j = \sum_{i=1}^N \mathbf{C}(\mathbf{r}_{ij}), \quad (36)$$

where $\mathbf{r}_{ij} = \mathbf{r}_i - \mathbf{r}_j$, and the summation ranges over $i \neq j$. \mathbf{C} is the disturbance tensor for just two particles, without the intervening effects of other particles. As it will turn out, the stress depends only on the divergence $\nabla \cdot [\mathbf{C} : \hat{\mathbf{\Gamma}}_s]$. The leading asymptotic form for large distances of this divergence is found by solving the two-particle creeping flow equations (with stick boundary conditions) [6,11],

$$\nabla_R \cdot [\mathbf{C}(\mathbf{R}) : \hat{\mathbf{\Gamma}}_s] = \frac{75}{2} \left(\frac{a}{R} \right)^6 \hat{\mathbf{R}} \cdot \hat{\mathbf{\Gamma}}_s \cdot \hat{\mathbf{R}}, \quad (37)$$

where $\hat{\mathbf{R}} = \mathbf{R}/R$ and a is the core radius of the colloidal particles.

The hydrodynamic force \mathbf{F}_j^h follows from the approximate force balance on the Brownian time scale. As a result of the large viscous friction of the core of the colloidal particles with the solvent, their momentum coordinates relax to equilibrium with the solvent in a very short-time interval. The Brownian time scale is larger than this momentum relaxation time. As a result, the total force on each colloidal particle is very small in comparison to each of the remaining forces on the Brownian time scale. There are three remaining forces: the hydrodynamic force \mathbf{F}_j^h , the potential interaction force

$-\nabla_j\Phi$, with Φ the total potential energy of the assembly of colloidal particles, and the Brownian force $-k_B T \nabla_j \ln\{P\}$, with P the probability density function of the position coordinates of all the colloidal particles. These forces add up zero on the Brownian time scale, and hence,

$$\mathbf{F}_j^h = \nabla_j \Phi + k_B T \nabla_j \ln\{P\}. \quad (38)$$

In this way the hydrodynamic force is expressed in terms of functions of the position coordinates of the colloidal particles.

The anomalous part of the viscoelastic response functions is found from the microscopic expression (34) together with Eqs. (35) and (38) to be equal to,

$$\left\{ \begin{array}{l} \eta' \\ \eta'' \end{array} \right\} = \frac{k_B T \bar{\rho}^{-2} C_s \omega}{\pi \dot{\gamma}_s} \int_0^{2\pi/\omega} dt \left\{ \begin{array}{l} \cos\{\omega t\} \\ \sin\{\omega t\} \end{array} \right\} \int_{R>d} d\mathbf{R} [h(\mathbf{R}) - h^{\text{stat}}(\mathbf{R})] \nabla_{\mathbf{R}} \cdot [\mathbf{C}(\mathbf{R}) : \mathbf{\Gamma}_s], \quad (39)$$

where $\bar{\rho} = N/V$ is the colloidal particle number density and C_s is a positive constant, which is related to the short-range behavior of the equilibrium correlation function. The average in the above result is with respect to $h - h^{\text{stat}}$, with h^{stat} the total-correlation function of the stationary sheared system, instead of just h , because in experiments only the oscillatory stress resulting from the superimposed flow is measured. The stress at zero superimposed shear rate $\lambda_s = 0$ is subtracted from the actual measured stress, which leads to subtraction of h^{stat} from the actual total-correlation function in Eq. (39).

Applying Parseval's theorem [see Eq. (8)], and the definition (6) of the structure factor, Eq. (39) can be written as,

$$\left\{ \begin{array}{l} \eta'(\lambda, \Omega, \xi^{-1}d) \\ \eta''(\lambda, \Omega, \xi^{-1}d) \end{array} \right\} = \eta_0 \frac{-C'}{(\xi^{-1}d)} \int d\mathbf{K} K_n^2 K_2 f(K\xi^{-1}d) \times \left\{ \begin{array}{l} F^{\text{in}}(\mathbf{K}|\lambda, \Omega) \\ F^{\text{out}}(\mathbf{K}|\lambda, \Omega) \end{array} \right\}, \quad (40)$$

where η_0 is the shear viscosity of the solvent, C' is a positive constant, d is the diameter of the colloidal particles, and the function f is a ‘‘cutoff function,’’ equal to,

$$f(x) = [(5x^5 - 10x^3 - 120x)\cos x + (5x^4 - 30x^2 + 120)\sin x] / (16x^5) - \frac{5}{16}x \int_x^\infty dz \frac{\sin z}{z}. \quad (41)$$

This function is equal to 1 for $x=0$, and is essentially 0 for $x>4$, thus limiting the integration range in Eq. (40) to small wave vectors, within the range of validity for which expressions for the structure factor have been given in the previous section.

In Ref. [9], Eq. (40) is written in terms of the ‘‘relative structure factor distortion’’ $(S - S^{\text{stat}})/S^{\text{eq}}$, instead of the functions $F^{\text{in,out}}$. The reason for introducing these functions

here is that they more clearly display the difference between parallel and orthogonal superposition. The relative structure factor distortion is different for both cases, but *the functions $F^{\text{in,out}}$ are the same for parallel and orthogonal superposition*. The only difference between orthogonal and parallel superposition is the factor K_n^2 in the wave vector integral in Eq. (40).

Since the structure factors are known, these expressions can be evaluated explicitly. Integrations must be done numerically.

D. Explicit results for the viscoelastic response functions

Since the functions $F^{\text{in,out}}$ are well-behaved at the critical point, by construction, and the cutoff function $f(x)$ tends to unity when $x \rightarrow 0$, the microscopic expression (40) predicts that the viscoelastic response functions diverge like the correlation length. This has been verified experimentally in case of response to a stationary shear flow in Ref. [12]. We therefore plot response functions multiplied by $\xi^{-1}d$, where the scaling results in a well-behaved function at the critical point. Furthermore we define the dimensionless response functions,

$$N'(\lambda, \Omega, \xi^{-1}d) \equiv \frac{1}{C'} \frac{\eta'}{\eta_0} \quad (42)$$

and similarly for N'' . The scaled response functions are plotted in Fig. 4 against the frequency for various values of the stationary Peclet number λ , and for $\xi^{-1}d = 0.01$, both for parallel and orthogonal superposition. The response functions for the otherwise quiescent system (with $\lambda = 0$) is virtually equal to the those with $\lambda = 0.1$, and are therefore not plotted. The storage and loss moduli $G' = \Omega N'$ and $G'' = \Omega N''$ are plotted in Fig. 5.

As can be seen, the response functions are not affected by the stationary component of the shear flow for frequencies $\Omega > 10\lambda$, approximately. Sufficiently fast diffusive modes are not affected by the stationary shear flow. Only the low-frequency part of the spectrum is affected on applying the stationary shear flow. At these low frequencies, N' is essentially constant, which plateau value decreases with increasing λ . Also, for these low frequencies N'' is almost 0 in the case of orthogonal superposition, while for parallel superposition N'' becomes negative. In the case of orthogonal superposition, N'' is only slightly negative, almost within the range of numerical accuracy. As far as we know, the first experimental observation of such negative values of response functions has been reported for polymer solutions by Laufer *et al.* [13].

Notice that the stress can be written as

$$\sigma(t) = \dot{\gamma}_s f(\omega) \cos\{\omega t - \varphi(\omega)\}, \quad (43)$$

where a positive phase angle φ implies a time lag of the stress response relative to the external field $\sim \cos\{\omega t\}$. Using that, $\cos\{\omega t - \varphi\} = \cos\{\varphi\}\cos\{\omega t\} + \sin\{\varphi\}\sin\{\omega t\}$, and comparing to Eq. (31) gives,

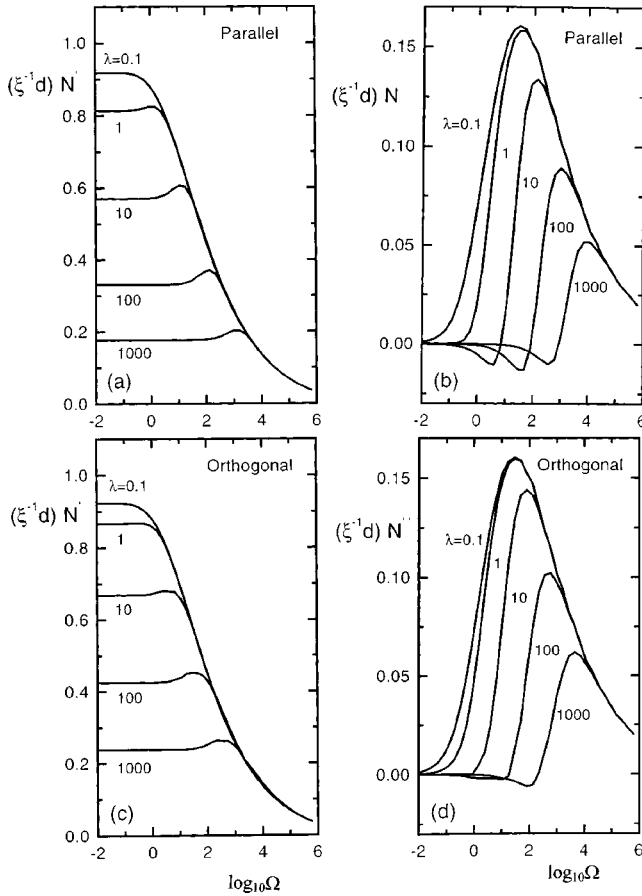


FIG. 4. The shear viscosity related to the superimposed shear flow (scaled with the factor $\xi^{-1}d$, which in the present case is equal to 0.01) as a function of the frequency on a logarithmic scale. The top two figures are for parallel superposition, the bottom two figures for orthogonal flow. (a) and (c) show the real part N' of the shear viscosity and (b) and (d) its imaginary part N'' . The various stationary Peclet numbers λ are indicated in the figures.

$$\eta'(\omega) = f(\omega) \cos\{\varphi(\omega)\},$$

$$\eta''(\omega) = f(\omega) \sin\{\varphi(\omega)\}. \quad (44)$$

Hence, a negative value of N'' , which continuously develops from a zero value at small frequencies, implies that the stress is actually ahead of the externally imposed field. This is not in contradiction with causality. In fact, the value of the structure factor in Eq. (23) at a given time depends only on past times, and is thus a causal solution. That the stress response is ahead of the external field is not in contradiction with causality since at times where transients have died away the system has experienced many oscillations and therefore ‘‘knows’’ about what is ‘‘ahead.’’ The future is just an infinite repetition of the past. At short times, when the external field just became active, there must be a time lag of the stress response, but as soon as transients died away, there is nothing against the stress being ahead of the external field.

It is also clear from Figs. 4 and 5 that for low frequencies ($\Omega < 10\lambda$, say) the response functions for parallel superposition are always smaller than for orthogonal superposition,

especially for larger values of the stationary Peclet number λ . The reason for this is as follows. As we have seen in Fig. 2, the structure factor response to the oscillatory shear component is roughly a factor of 10 smaller for the parallel case in comparison to orthogonal superposition. This is caused by the fact that part of the equilibrium microstructure is unaffected by the stationary shear flow: in directions perpendicular to the stationary flow the structure factor is equal to the equilibrium structure factor [see Eq. (28) and Fig. 1]. For parallel superposition the external field just modifies the shear rate of the stationary flow a bit, and the structure factor perpendicular to the flow direction remains equal to the equilibrium structure. *For parallel superposition, only the microstructure that is already distorted by the stationary flow is probed.* For orthogonal superposition, however, the structure that is unaffected by the stationary flow will also be affected. *For orthogonal superposition, part of the microstructure that is probed is the equilibrium microstructure.* Since the non-distorted, equilibrium microstructure is more susceptible to an external field than the already highly distorted microstructure, orthogonal response functions are larger than parallel response functions. This is the reason why, for example, the storage modulus for parallel superposition goes down with decreasing frequencies much faster as for orthogonal superposition [see Figs. 5(b) and 5(d)].

Within the present microscopic approach, *the difference between the viscoelastic response for orthogonal and parallel superposition is entirely due to the anisotropy in microstructural order under stationary shear flow.* Our reasoning is entirely based on the anisotropy of the stationary sheared structure factor. Such an input is completely absent in phenomenological models for superposition rheology and seems to obscure the connection between the two approaches.

For the near-critical system discussed above, the dominant effect of the stationary shear flow is to diminish microstructural order. This may be different in more complicated systems, like entangled polymers. Here, stationary shear flow can induce a considerable amount of new microstructure. This new microstructure does of course respond to the superimposed oscillatory shear flow and can thus lead to an increase of the response as compared to the otherwise quiescent system. This might even lead to larger parallel response as compared to orthogonal response.

V. ON THE VALIDITY OF THE KRAMERS-KRONIG RELATIONS

Let us first recapitulate the conditions under which the Kramers-Kronig relations are valid. Define a response function $\hat{f}(\Omega)$, with $\Omega \in \mathfrak{R}$, as,

$$\hat{f}(\Omega) = \int_0^\infty d\tau f(\tau) \exp\{i\Omega\tau\}. \quad (45)$$

The fact that the integration ranges from 0 to ∞ instead of the entire real axis expresses causality. We impose the condition,

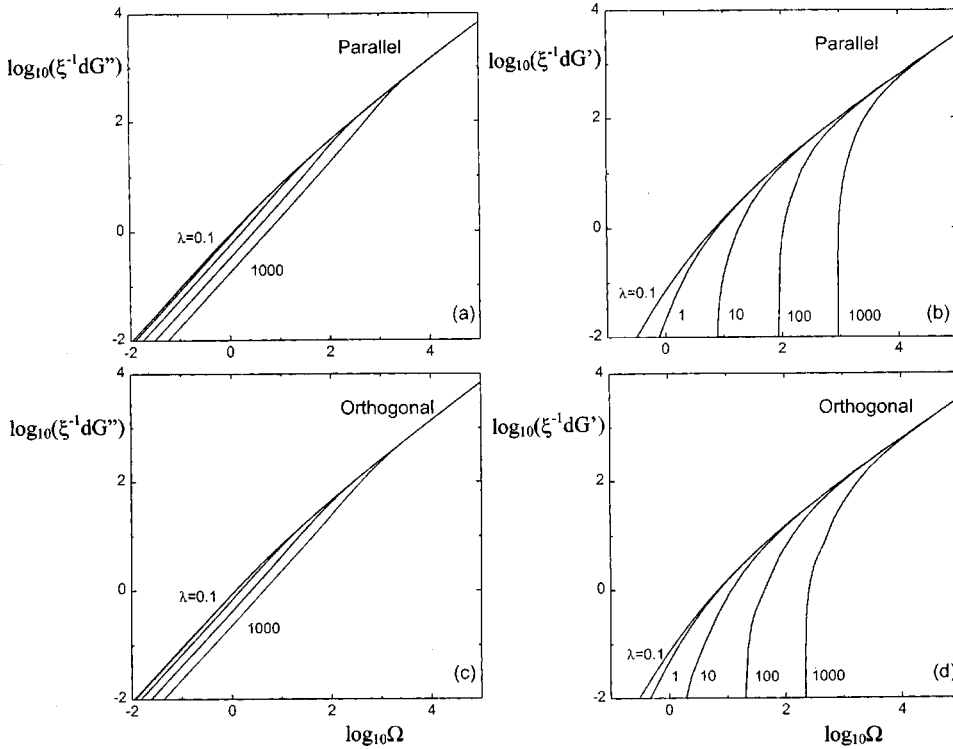


FIG. 5. The loss and storage moduli (scaled with the factor $\xi^{-1}d$, which in the present is equal to 0.01) as a function of the frequency on a double-logarithmic scale. The top figures are for parallel superposition, the bottom two for orthogonal flow. (a) and (c) show the loss moduli and (b) and (d) the storage moduli. The various stationary Peclet numbers λ are indicated in the figures (for the two left figures the values of λ for the various curves are the same as for the two figures on the right).

$$\int_0^{\infty} d\tau \tau |f(\tau)| < \infty, \quad (46)$$

on $f(\tau)$. It would be physically unrealistic when $f(\tau)$ would be singular for some finite-time τ . The possible divergence of the above integral can therefore only be due to a too slow decay of $|f(\tau)|$ to 0 as $\tau \rightarrow \infty$. This condition thus implies that,

$$\int_0^{\infty} d\tau |f(\tau)| < \infty. \quad (47)$$

The two above conditions (46) and (47) imply that $\hat{f}(\Omega)$ is continuous differentiable on the real axis, and allow to continue this function analytically into the upper half of the complex plane. This analytic continuation is obtained by replacing Ω in Eq. (45) by the variable $z = x + iy$ with x and y both real, while $y \geq 0$ in the upper half of the complex plane. We simply denote this analytic continuation as $\hat{f}(z)$. Let $C^+(R) = \{z | z = R \exp\{i\varphi\}, \varphi \in [0, \pi]\}$ denote the semicircle with radius R in the upper half plane. Whenever $\hat{f}(z)$ vanishes on the semicircle when the radius tends to infinity, that is, when,

$$\lim_{R \rightarrow \infty} \max_{\varphi \in [0, \pi]} |\hat{f}(z = R \exp\{i\varphi\})| = 0, \quad (48)$$

the integral of $\hat{f}(z)/(z - \Omega)$ with respect to z over the curve $C^+(R)$ tends to 0 when $R \rightarrow \infty$. The Kramers-Kronig relations now follow directly from Cauchy's integral theorem. The Eqs. (46)–(48) are thus sufficient conditions for the va-

lidity of the Kramers-Kronig relations for the real and imaginary parts of the function \hat{f} defined in Eq. (45). In fact, assuming continuity of $f(\tau)$, the inequality (46) implies the inequality (47), so that the actual conditions to be satisfied are Eq. (46) and (48).

For the colloidal system under consideration here, we have from Eqs. (30) and (40),

$$\eta(\Omega) = \eta'(\Omega) + i\eta''(\Omega) = \int_0^{\infty} d\tau f(\tau) \exp\{i\Omega\tau\}, \quad (49)$$

where,

$$\begin{aligned} f(\tau) = & \eta_0 \frac{-C'(\xi^{-1}d)}{\lambda} \int d\mathbf{K} \frac{K_n^2 K_2}{K_1} f(K\xi^{-1}d) \\ & \times G^2(\tau) [1 + G^2(\tau)] \{S^{\text{stat}}(\mathbf{G}(\tau)) - S^{\text{eq}}(\mathbf{G}(\tau))\} \\ & \times \exp\{-H(\tau)\}. \end{aligned} \quad (50)$$

Let us analyze whether the two conditions (46) and (48) are satisfied for the present case.

Consider first the condition (46), which is a condition on the long-time behavior of $f(\tau)$; this function should decay to zero at infinity sufficiently fast to guarantee the existence of the integral. The long-time behavior of $f(\tau)$ relates to the small frequency behavior of $\hat{f}(\Omega) \equiv \eta(\Omega)$. Now suppose that the effect of the stationary shear is to diminish the microstructure, that is, the structure factor under stationary shear is smaller than the equilibrium structure factor for all wave vectors. In that case the response functions to a superimposed flow at low frequencies are smaller than the re-

sponse functions of the otherwise quiescent system; part of the microstructure that could have responded is now destroyed by the stationary shear flow, or equivalently, structure that would have responded in the absence of stationary shear flow is no longer available for superimposed response. In that case the response function $|f(\tau)|$ cannot be larger than for the otherwise quiescent system. This implies that the condition (46) is satisfied for the superimposed response functions whenever it is satisfied for the otherwise quiescent system.

Furthermore, the response function $\eta(\Omega)$ will not be affected by the stationary shear flow for sufficiently large frequencies of the superimposed flow, since sufficiently fast dynamical modes are able to instantaneously follow the external field. In fact, as we have seen in Sec. IVD (see in particular Figs. 4 and 5), the viscosity is not affected for frequencies larger than about 10λ . Hence, when the condition (48) for $\hat{f}(z) \equiv \eta(z)$ is satisfied without stationary shear flow, they are also satisfied in the presence of a stationary shear flow.

The conclusion from the above reasoning is, that when the Kramers-Kronig relations hold for the usual frequency dependent viscosity where no stationary shear field is applied, they also hold for the viscosity related to a superimposed oscillatory flow.

The crucial assumption that was made to arrive at the validity of the Kramers-Kronig relations, was that the structure factor is diminished by the stationary flow for all wave vectors. Even for the near-critical system considered here this is not entirely true. Along the compressional direction of the shear flow there is an increase of the structure factor. The breakdown of structure is however much more dominant, so that the arguments given above remain valid. There are systems, however, for which there is a considerable enhancement of structure due to the stationary shear flow, such as entangled polymer systems and colloidal systems close to a gel line. It might be that for such systems the Kramers-Kronig relations are violated.

VI. REMARKS AND CONCLUSION

In the present microscopic approach the difference between parallel and orthogonal response functions can be understood entirely on the basis of the anisotropic microstructure under stationary shear flow. Particularly important is the fact that the stationary flow does not affect the microstructure in directions perpendicular to the flow direction. In these directions the structure factor remains the same as in equilibrium [see Fig. 1 and Eq. (28)]. Under a parallel superimposed flow, the structure factor retains its equilibrium form in directions perpendicular to the flow, and only modifies the distortion that is already caused by the stationary flow. The still existing equilibrium structure that is present under stationary flow will be probed, however, by an orthogonal superimposed flow field. Hence, *parallel superposition probes nonequilibrium structure only while orthogonal superposition probes also in part, equilibrium structure.*

A generally valid statement is that *the difference between the response to parallel and orthogonal superposition is due*

to the fact that the stationary sheared microstructure is anisotropic, and the two superposition experiments probe different parts of this anisotropic structure. The parallel superposition response functions will generally be larger than the orthogonal ones, since parallel superposition probes already highly distorted microstructure (by the stationary flow), while orthogonal superposition probes microstructure that is distorted to a lesser extent.

For the systems discussed here, superimposed response functions are found to be smaller than the response functions for the otherwise quiescent system, where stationary shear flow is absent. This is due to the fact that the breakdown of microstructural order is dominant over shear induced order. For more complicated systems, like entangled polymer solutions or systems close to the gel transition line, stationary shear flow may induce a considerable amount of new structure. This new microstructure, that does not exist without stationary shear flow, can lead to an enhancement of the response functions; new microstructure is created that can respond to the superimposed flow. In such cases superimposed response functions can be larger for sufficiently small frequencies as compared to the response functions for the otherwise quiescent system.

The Kramers-Kronig relations hold when the breakdown of microstructure due to the stationary flow is dominant over the stationary shear enhancement of microstructure. In such cases the inequality (46) is satisfied, which ensures the validity of the Kramers-Kronig relations. There are a number of phenomenological models that do not satisfy the Kramers-Kronig relations. This does not mean that these phenomenological models are inaccurate; it can very well be that, at least within some frequency range, these models give accurate estimates for response functions. However, it would be reassuring when a phenomenological model does satisfy the Kramers-Kronig relations. A purist might say that such models that violate the Kramers-Kronig relations are “fundamentally wrong,” while a practitioner might say that they are “quite accurate in the experimentally accessible frequency range.” *The Kramers-Kronig relations could be violated for systems where the stationary shear flow induces a considerable amount of new structure, like entangled polymers or systems close to the gel transition line.*

One of the important points here has been that the structure factor is not affected by shear flow in directions perpendicular to the flow direction [see Eq. (28)]. An exact numerical treatment of the two-particle Smoluchowski equation for hard spheres [14] shows that the distortion along these directions is nonzero. This is due to nonlinear terms in the equation of motion for the total-correlation function and to the no-flux condition at contact of two particles. For the present case of colloids near their gas-liquid critical point, however, the situation is quite different: linearization is allowed in the mean-field region, while the no-flux condition plays no role here, since the asymptotic behavior of the total-correlation function for large distances is calculated. Indeed it has been shown experimentally [15] that there is no distortion of the structure factor in directions perpendicular to the flow direction, except very close to the critical point, beyond the mean-field region.

- [1] J. Vermant, L. Walker, P. Moldenaers, and J. Mewis, *JNFFM* **79**, 173 (1990).
- [2] R.I. Tanner, *Trans. Soc. Rheol.* **12**, 155 (1968).
- [3] S. Hess, *Physica A* **87**, 273 (1977).
- [4] J.M. Deutch and I.J. Oppenheim, *J. Chem. Phys.* **54**, 3547 (1971).
- [5] T.J. Murphy and J.L. Aguirre, *J. Chem. Phys.* **57**, 2098 (1972).
- [6] J.K.G. Dhont, *An Introduction to Dynamics of Colloids* (Elsevier, New York, 1996), Chap. 4.
- [7] G.K. Batchelor, *J. Fluid Mech.* **41**, 545 (1970); **83**, 97 (1977).
- [8] H.E. Stanley, *Introduction to Phase Transitions and Critical Phenomena* (Oxford University Press, Oxford, 1971), Chap. 7.
- [9] J.K.G. Dhont, *J. Chem. Phys.* **103**, 7072 (1995).
- [10] J.K.G. Dhont and G. Nägele, *Phys. Rev. E* **58**, 7710 (1998).
- [11] G.K. Batchelor and J.T. Green, *J. Fluid Mech.* **56**, 375 (1972).
- [12] I. Bodnár and J.K.G. Dhont, *Phys. Rev. Lett.* **77**, 5304 (1996).
- [13] Z. Laufer, H.L. Jalink, and A.J. Staverman, *Rheol. Acta* **14**, 641 (1975).
- [14] J. Bławdziewicz and G. Szamel, *Phys. Rev. E* **48**, 4632 (1993).
- [15] J.K.G. Dhont and I. Bodnár, *Phys. Rev. E* **58**, 4783 (1998).